Applied Clay Science 118 (2015) 124–130

Contents lists available at ScienceDirect

Applied Clay Science

journal homepage: www.elsevier.com/locate/clay

Structural, textural and acidic properties of Cu-, Fe- and Cr-doped Ti-pillared montmorillonites

B. González-Rodríguez [a], R. Trujillano [a], V. Rives [a], M.A. Vicente [a,*], A. Gil [b], S.A. Korili [b]

[a] GIR-QUESCAT, Departamento de Química Inorgánica, Universidad de Salamanca, 37008 Salamanca, Spain
[b] Departamento de Química Aplicada, Universidad Pública de Navarra, 31006 Pamplona, Spain

ARTICLE INFO

Article history:
Received 7 July 2015
Received in revised form 10 September 2015
Accepted 11 September 2015
Available online 20 September 2015

Keywords:
Montmorillonite
Titanium
Ti-PILC
Doped pillared clays

ABSTRACT

Montmorillonite has been treated with Ti-based solutions, alone or doped with Cu^{2+}, Fe^{3+} or Cr^{3+} cations, yielding new intercalated solids, which have been calcined at various temperatures to test the stability of the so-formed pillars. The solids calcined at 500 °C were fully characterized by chemical analysis, X-ray diffraction, FT-IR spectroscopy, thermal analyses, nitrogen adsorption and acidity evaluation. The evolution of the specific surface area, porosity and acidic properties is discussed, analysing the effect of pillaring and doping procedures on these properties.

1. Introduction

Montmorillonite (Mt) a layered clay mineral behaving to the smectite group is able to absorb or exchange cations or molecules between the layers and on the external surface. This is favoured by the easy swelling of this clay mineral. The applicability of the smectites modified by different treatments in the chemical industry and environmental protection has been largely studied and reported in the literature (Harvey and Lagaly, 2013; McCabe and Adams, 2013; Yuan et al., 2013).

An important disadvantage of smectites is the difficulty of controlling a permanent interlayer space, as their dehydration at 250 °C gives rise to the collapse of the layers, which makes the interlayer space inaccessible, limiting their applicability. The intercalation of large polyoxometalates and the subsequent calcination of the intercalated solids thus obtained give rise to stable structures with constant interlayer space up to high temperatures. This process, called pillaring, allows one to obtain solids with the adequate porosity to be used in catalysis applications (Gil et al., 2010; Vicente et al., 2013). It has been shown that the pillars constitute the most active phase in these solids, while the layers mainly act as supports for this ultradispersed phase.

TiO_2 is the most popular photocatalyst, showing optimum properties, as high performance, low cost, chemical inertness, photostability, and biocompatibility (Schneider et al., 2014), being largely used in the degradation of pollutants by photocatalysis (Nakata and Fujishima, 2012; Barbosa et al., 2015). TiO_2 can be incorporated to smectites by pillaring, and in some cases higher activity has been reported for Ti-pillared clays than for TiO_2 powder particles, as pillared clays stabilize TiO_2 particles and allow the reactant molecules to access to the surface of TiO_2 crystals (Kocí et al., 2011). Recently, incorporation of Ti to clays forming porous clay heterostructures, PCH, has been reported (Chmielarz et al., 2009), while it can be expected that the addition of small amounts of doping cations may enhance the activity of titania-pillared materials.

The aim of this work is to incorporate doping cations into titanium-pillared montmorillonite, and to study the changes in the structural, textural and surface properties compared to the undoped titanium-pillared montmorillonite. In order to reach this target, Ti-solutions were doped with Fe^{3+}, Cr^{3+} and Cu^{2+} before the polymerization step, allowing a later incorporation of these metals to the final titanium-Mt pillared nanocomposite. The incorporation of these metals and their influence on the properties of the final solids is discussed.

2. Synthesis procedure and characterization techniques

The clay mineral used in this work was a raw montmorillonite from Cheto, Arizona, USA (The Clay Minerals Repository, where this sample is denoted as SAz-1). The natural clay mineral was purified before its use by dispersion–decantation, separating the ≤2 μm fraction. In the present work, this clay is designated as "Mt". Its cation exchange capacity was 0.67 meq/g, its basal spacing 13.60 Å and its BET specific surface area 49 m^2/g.

The preparation of the Ti-pillared Mt was carried out adapting the method proposed by Lin et al. (Lin et al., 1993). The Ti-polycation solution was prepared by slow addition, under vigorous stirring, of 11 mL of $TiCl_4$ (Sigma-Aldrich) to 22 mL of absolute ethanol (Panreac), until a

* Corresponding author.
E-mail address: mavicente@usal.es (M.A. Vicente).

http://dx.doi.org/10.1016/j.clay.2015.09.010
0169-1317/

homogeneous yellowish solution was obtained. A portion of 8 mL of the resulting solution was then added to a previously prepared solution of 25 mL of glycerine (Panreac) in 25 mL of distilled water. The new mixture was maintained under stirring for 3 h. Under these conditions, $[(TiO)_8(OH)_{12}]^{4+}$ is claimed to be the titanium polycationic species formed (Einaga, 1979). This intercalating solution was added dropwise to a previously prepared clay suspension, with a Ti/clay ratio of 40 mmol/g, ageing the new suspension under magnetic stirring for 18 h. Then, the solid was separated by centrifugation, washed by dialysis for 2 days, dried overnight at 70 °C and finally calcined at 500 °C for 2 h, at a heating rate of 1 °C/min. This solid was designated as MtTi. For comparative purposes, the intercalated Mt was also calcined at 300 °C, when necessary these solids will be identified by adding the temperature of calcination to their names.

In the case of the doped solutions, the appropriate amount of doping cations, Fe^{3+}, Cr^{3+} and Cu^{2+}, were added to the $TiCl_4$ solution, using two ratios between Ti^{4+} and the doping cations, namely, 90:10 and 95:5. $CrCl_3 \cdot 6H_2O$, ferric citrate and $Cu(NO_3)_2 \cdot 3H_2O$ were used as precursor salts. The rest of the preparation procedure was the same described for the Ti-solid. The solids were designated adding the symbol of the doping cation and its percent amount, i.e., MtTiCr10 is the Mt treated with a solution containing 10% Cr^{3+} and 90% Ti^{4+}.

Element chemical analyses were carried out at Activation Laboratories Ltd., in Ancaster, Ontario, Canada, using inductively coupled plasma-atomic emission spectrometry (ICP-AES). X-ray diffraction (XRD) patterns were recorded between 2 and 70° (2θ) over non-oriented powder samples, at a scanning speed of 2°/min, by using a Siemens D-500 diffractometer, operating at 40 kV and 30 mA, and filtered Cu Kα radiation (λ = 1.5418 Å). FT-IR spectra were recorded in the 450–4000 cm^{-1} range in a PerkinElmer Spectrum-One spectrometer by the KBr pellet method (sample: KBr ratio 1:300). Thermal analyses were performed on a SDT Q600 TA instrument, both analyses were carried out simultaneously; all measurements were carried out under a flow of 20 mL/min of oxygen (L'Air Liquide, Spain, 99.999%) and a temperature heating rate of 10 °C/min from room temperature to 900 °C. Textural properties were determined from nitrogen (L'Air Liquide, 99.999%) adsorption–desorption data, obtained at −196 °C using a Micrometrics Gemini VII 2390 t, Surface Area and Porosity apparatus. Specific surface area (SSA) was obtained by the BET method, external surface area and micropore volume by means of the t-method, and the total pore volume from the nitrogen adsorbed at a relative pressure of 0.95 (Brunauer et al., 1938; Lippens and de Boer, 1965; Rouquerol et al., 1998).

The acidity of the solids was evaluated by adsorption of pyridine and further heating at increasing temperatures, following the process by FTIR spectroscopy. The solids (20 mg) were exposed to pyridine vapour in a desiccator, under vacuum for one hour. Then, wafers for FTIR were prepared using a sample: KBr ratio of 10:600. The spectra were recorded after outgassing under vacuum at room temperature, and after heatings for 1 h at 100, 200 and 300 °C, in each case followed by cooling under vacuum. The spectra were recorded using the spectrometer above described. The number of Brönsted and Lewis acid sites was evaluated by means of the following equation, proposed by Barzetti et al. and successfully applied to clay materials by Del Rey Pérez-Caballero and Poncelet (Barzetti et al., 1996; Del Rey-Pérez-Caballero and Poncelet, 2000):

$$q_{B,L} = \frac{A_{B,L}\pi R^2}{\omega \varepsilon_{B,L}}$$

where $q_{B,L}$ is the concentration (μmol/g) of Brönsted or Lewis acid sites, R is the radius of the wafer (cm), ω is the wafer mass (g), and $A_{B,L}$ is the integrated area of the bands at 1545 cm^{-1} (for Brönsted sites) and 1450 cm^{-1} (for Lewis sites). For the extinction coefficients, $\varepsilon_{B,L}$, the values reported by Emeis were used, 1.67 ± 0.12 cm/μmol and 2.22 ± 0.21 cm/μmol, for Brønsted and Lewis sites, respectively (Emeis, 1993).

3. Results and discussion

The chemical composition of the raw Mt. is given in Table 1, being a composition typical for this clay mineral. From this composition, the following structural formula can be calculated:

$$[Si_{8.00}]\,[Al_{2.717}Fe_{0.153}Mg_{1.206}Mn_{0.005}Ti_{0.026}]\,O_{20}(OH)_4[Ca_{0.262}Na_{0.017}K_{0.011}].$$

The chemical compositions of the Ti pillared Mt are also given in Table 1. Some points may be highlighted about the composition of the treated solids. Thus, the amount of Ti fixed was close to 15%, expressed as TiO_2, while the doping elements were fixed in all cases in low extend. The incorporation of the pillaring elements was carried out by cationic exchange of Ca^{2+}, which almost disappeared from the solids, and in much lower extent, of Na^+ and K^+, which were in very low amounts in the original Mt. The incorporation of the pillaring elements produced an important relative decrease in the amount of the other components. The amount of TiO_2 fixed showed important differences between the samples, and although the solids were stored under similar conditions, the amount of water in them was very different, the sum of the metal oxides varying between 56 and 81%. To evidence the modifications caused in the chemical composition by the fixation of Ti, a double normalization was carried out. First, the amount of the metal oxides was normalized to a total of 100%, thus avoiding the presence of several amounts of water (water-free solids). Secondly, the compositions were referred to the amount of SiO_2 in the original Mt, assuming that the tetrahedral sheet of the Mt was not altered by the treatments carried out and that SiO_2 can be used as a sort of "internal standard". The compositions thus normalized are given in Table 2.

When comparing the normalized compositions, it can be observed that the amount of TiO_2 fixed by the solids was very similar, being, once subtracted the amount of TiO_2 present in the raw Mt., between 23.60 and 26.01% (about 9–10% of the titanium existing in the initial solution).The amounts of Al_2O_3 and Fe_2O_3 remained practically constant, while that of MgO slightly decreased, from 6.91 to 6.70%. These results strongly suggested that the incorporation of TiO_2 took place without modifying the chemical composition of the Mt. layers; in spite of the relatively strong conditions needed for Ti-polymerization, octahedral Al^{3+} and Fe^{3+} were not at all dissolved, and Mg^{2+} was dissolved in a very small amount (even, part of the dissolved Mg^{2+} should be in the original solid as exchangeable cation). Almost all Ca^{2+} and a small amount of Na^+, present as exchangeable cations, were removed, while K^+ remained constant, probably it was associated to an insoluble impurity, as feldspar.

As indicated above, $[(TiO)_8(OH)_{12}]^{4+}$ has been proposed to be formed upon polymerization of Ti^{4+}, in this species each Ti atom has a formal charge of +0.5 (Einaga, 1979). If all the titanium incorporated into the clay was in this form, the number of polycations in MtTi solid would be 0.27 per formula unit, balancing 1.08 charges, almost double of the CEC of the clay. More precisely, assuming that the Ti incorporated to the clay balances the charge of the cations Ca^{2+} and Na^+ effectively exchanged, the average charge of each Ti atom would be +0.24. This suggested that the polymerization of titanium lead to species with higher polymerization degree or, alternatively, considering the difficult polymerization of this element, that part of Ti may be incorporated to the solid as small precipitated particles of amorphous TiO_2.

The composition of the pillared solids containing doping elements is also summarized in Table 1, and after normalization to the content of SiO_2, in Table 2. First of all, it may be remarked that the presence of a doping element increased, in all cases, the amount of titanium fixed to the solids, between 0.3 and 2.4% higher in the doped solids than in MtTi. At the same time, the amount of the doping elements fixed in the solids was low; in the cases of Cr and Cu, the amount fixed was directly observed in the chemical analyses, while in the case of Fe, it may be obtained after subtracting the amount of this element in the raw clay, the amounts fixed being 0.09 and 0.22% of Fe_2O_3 for samples

Table 1
Chemical composition of the solids, expressed in content of their metallic oxides (mass percentage).

	SiO_2	Al_2O_3	Fe_2O_3	MnO	MgO	CaO	Na_2O	K_2O	TiO_2	Cr_2O_3	CuO	Total
Mt	55.8	15.92	1.41	0.043	5.58	1.69	0.06	0.06	0.21			80.78
MtTi	43.72	12.7	1.13	0.004	4.25	0.03	0.03	0.04	15.10			77.00
MtTiFe5	43.84	12.65	1.17	0.004	4.24	0.03	0.02	0.04	15.43			77.42
MtTiFe10	33.27	9.78	0.95	0.004	3.23	0.06	0.02	0.03	12.63			59.97
MtTiCu5	43.48	12.41	1.12	0.004	4.22	0.03	0.02	0.05	15.43		0.02	76.78
MtTiCu10	33.58	9.66	0.87	0.004	3.25	0.06	0.02	0.03	12.77		0.25	60.49
MtTiCr5	31.15	9.1	0.82	0.014	3.04	0.07	0.02	0.03	11.56	0.09		55.89
MtTiCr10	34.11	9.89	0.88	0.019	3.32	0.06	0.02	0.03	12.30	0.15		60.78

MtTiFe5 and MtTiFe10, respectively. The amount of the doping metals incorporated into the solids increased when their amount in the precursor solutions also increased. However, the amount fixed was always very far from the amount existing in solution.

Ions Cr^{3+} and Fe^{3+} can polymerize themselves forming polycationic species (Stünzi and Marty, 1983; Rightor et al., 1991), while, up to our best knowledge, polymerization of Cu^{2+} has not been reported. However, the conditions needed for the polymerization of Cr^{3+} and Fe^{3+} are far from those here used for favouring polymerization of Ti^{4+}. These cations may be incorporated into the Ti-polycationic species, as their ionic radii are only slightly higher than that of Ti^{4+} (Greenwood and Earnshaw, 2012). However, this has not been reported in the literature and no evidence has been found in the present work, and the formation of segregated species may also be proposed. It is remarkable that although their fixation degree was very low, the presence of the doping elements significantly affected the polymerization of Ti^{4+}, leading to the mentioned increase in the amount of this element incorporated to the solids.

As indicated, all the solids contained ca. 25% of TiO_2, and small amounts of the doping elements in the solids from the doped series. So, the solids are formed by ca. three parts of clay and one of (doped)-TiO_2.

The powder X-ray diffractograms of some representative solids are shown in Fig. 1, and the basal spacing of all the solids are summarized in Table 3. The raw solid was a well-ordered Mt with a basal spacing of 13.60 Å. The treatment with the intercalating solutions always led to the expansion of the interlayer region, the basal spacing varying between 18.9 and 22.9 Å for the intercalated, dried solids. The intercalated solids were well ordered, and their 002 reflection was clearly observed, with high intensity, in some of the solids. MtTi showed high basal spacing, 18.80 Å, which indicated that Ti-polycations were intercalated in the interlayer region in a cationic form by an exchange mechanism, although the incorporation of some neutral species or disperse particles cannot be ruled out. The 001 reflection was less intense for MtTi than for the M solid, indicating that the intercalation process decreased the layer ordering, MtTi being almost completely delaminated. Reflections belonging to the in-layer reflections, independent of *c*-stacking, were recorded at the same positions for all the solids, indicating that the layers were not modified. The stacking degree decreased as the calcination temperature increased but the basal spacings remained almost constant. The solid calcined at 300 °C was grey in colour, this colour disappeared when calcining at 500 °C, this temperature being necessary for the complete removal of the organic residues from the intercalation reactants. No reflection belonging to crystalline TiO_2 or other metal oxides containing Ti was observed.

For the doped solids, some interesting effects were observed. In most of the cases, the basal spacing of the co-intercalated solids is higher than that of MtTi, up to 3.2 Å higher. In all cases, the basal spacing of the intercalated solids increased when the amount of the doping element increased from 5 to 10%, and in this last case, the *c*-axis ordering was largely improved, and 002 reflections were clearly observed in the XRD diagrams of all solids. All the solids remained ordered when calcined at 300 °C, but the structure collapsed in all the solids belonging to 5% series when calcined at 500 °C, while remained ordered at this temperature for the solids belonging to 10%-doping metal series (it may be taken into account that although 5 and 10% were the nominal contents of the doping metals in the intercalating solutions, the amount fixed by the solids was always much smaller). However, these solids had basal spacing between 16.03 and 16.99 Å, always lower than the spacing of the Ti-PILC (18.60 Å). It may be remarked that not simple or mixed phases involving the doping elements were detected in the final solids by X-ray diffraction.

These significant effects on the final properties of the pillared solids may reasonably be attributed to changes in the polymerization of Ti. Obviously, an increase of 3.2 Å in the size of the polycations cannot be explained by the isomorphous incorporation of the doping elements, even if they are slightly larger than Ti^{4+}. The larger basal spacings of the intercalated solids in these series suggested that the presence of Fe^{3+}, Cr^{3+} or Cu^{2+}, less acidic that Ti^{4+}, may significantly affect its polymerization, giving rise to larger polycations that when Ti^{4+} polymerized by itself. The larger size of the polycations may also be related to the presence of high water content, easily removed in the calcination step, giving rise to smaller pillar heights than when Ti^{4+} polymerized alone. Besides of the size of the polycations, their thermal resistance was also remarkable, as while it was very low in the 5% series, it was higher than that of only-containing Ti solutions for 10% series.

The FT-IR spectra of MtTi and the doped samples were rather similar to that of natural Mt, as it could be expected (Figure S1). Stretching O–H and bending H–O–H vibrational modes were recorded around 3426 and 1627 cm^{-1}, respectively. Bands corresponding to the in-layer Si–O–Si and Si–O–Al vibrations were recorded at 1050 and 473 cm^{-1}. No M–O (M = Ti, Fe, Cu or Cr) bands were observed for the intercalated clays. Some of the characteristic vibrations of the clay showed significant changes during intercalation. The intensity of the O–H stretching

Table 2
Chemical composition of the water-free solids, normalized to the SiO_2 content in the raw montmorillonite (mass percentage).

	SiO_2	Al_2O_3	Fe_2O_3	MnO	MgO	CaO	Na_2O	K_2O	TiO_2	Cr_2O_3	CuO
Mt	69.08	19.71	1.75	0.05	6.91	2.09	0.07	0.07	0.26		
MtTi	69.08	20.07	1.79	0.01	6.72	0.05	0.05	0.06	23.86		
MtTiFe5	69.08	19.93	1.84	0.01	6.68	0.05	0.03	0.06	24.31		
MtTiFe10	69.08	20.31	1.97	0.01	6.71	0.12	0.04	0.06	26.22		
MtTiCu5	69.08	19.72	1.78	0.01	6.70	0.05	0.03	0.08	24.51		0.03
MtTiCu10	69.08	19.87	1.79	0.01	6.69	0.12	0.04	0.06	26.27		0.51
MtTiCr5	69.08	20.18	1.82	0.03	6.74	0.16	0.04	0.07	25.64	0.20	
MtTiCr10	69.08	20.03	1.78	0.04	6.72	0.12	0.04	0.06	24.91	0.30	

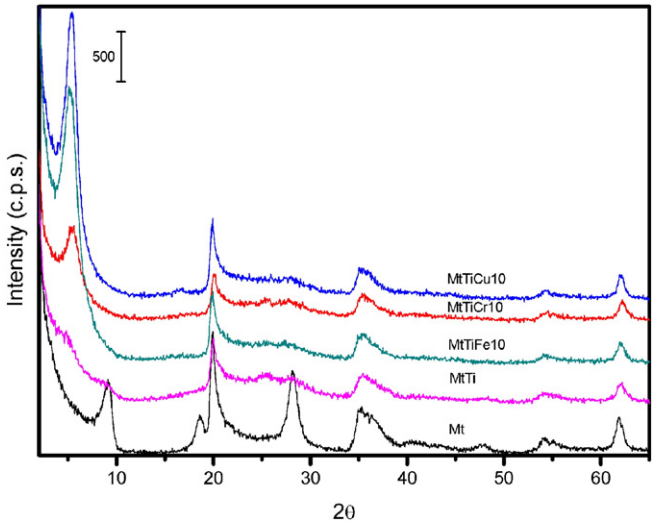

Fig. 1. X-ray diffractograms of the pillared solids calcined at 500 °C.

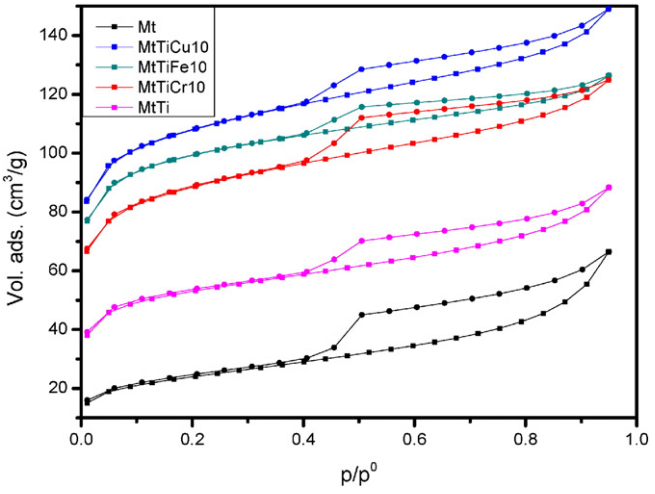

Fig. 2. Nitrogen adsorption–desorption isotherms of the pillared solids calcined at 500 °C.

mode of the hydroxyls bonded to the metals, recorded around 3600 cm^{-1}, increased after intercalation, showing the interaction of these groups with the polycations. The band characteristic of the tetrahedral layer slightly shifted about 10 cm^{-1} towards larger wavenumbers, which can be attributed to the removal of some octahedral cations, especially Mg^{2+}, under the acidic conditions used for intercalation. In fact, this shift is typical of acid activation of clays, where displacements of up to 100 cm^{-1} have been reported when the treatment is severe, and implies a change in the atomic sequence from Si–O–M–O–Si (M = Mg, Al or Fe), characteristic of the clay, to Si–O–Si–O–Si, typical of amorphous silica (Vicente Rodríguez et al., 1996). For the samples calcined at 500 °C, the intensities of water and hydroxyl related vibrations strongly decreased, the Al–OH disappeared, and the Si–O–Mg band at 473 cm^{-1} was well defined. No bands involving the doping cations were detected.

The thermogravimetric curve for MtTi solid showed a 7% mass loss at low temperature, associated to an endothermic effect centred at 50 °C in the DTA curve. This effect was attributed to the removal of interlayer water or that adsorbed on the surface of the sheets. In the central temperature range, a significant mass loss effect (10%) was observed, with three slight inflexions, associated to an exothermic effect centred at 270 °C and a shoulder at 370 °C, and attributed to the combustion of the organic chain of the precursor. Removal of structural hydroxyls and the phase change to form mullite was observed close to 860 °C. The total mass loss is close to 20%. DTA and TG curves for doped solids were very similar to those for the MtTi solid; the incorporation of the small amounts of the doping elements did not produce significant changes in the curves (Figure S2).

The textural properties of the solids were studied by means of N_2 adsorption–desorption isotherms. The isotherms belonged to type II from IUPAC classification, with a H4 type hysteresis loop at high relative pressures, which is associated to narrow slit pores (Fig. 2). The loop had an inflexion at a relative pressure value of 0.4, being reversible at low p/p^0 values for the non-calcined solids, indicate that pores were not rigid but flexible, and become practically reversible for the calcined solids. t-plots of the calcined doped solids had two well differentiated regions, the first one showed a positive intercept with the adsorption axis when extrapolated to t = 0, while the second portion had a lower slope. The curvature between the two linear portions indicated a broad distribution of micropore size.

BET specific surface area, external surface area and micropore volume data are summarized in Table 4. Natural Mt had a low SSA value, 49 m^2/g. This solid was calcined at 500 °C, under the same conditions used for the preparation of the pillared solids, and SSA value increased to 80 m^2/g. In the case of the MtTi solid, the evolution of SSA was analysed as a function of the temperature. The as-intercalated solid had a SSA of 97 m^2/g, indicating that although the basal spacing strongly increased by the incorporation of the polycations, most of this space was occupied by the polycations themselves. This fact, together with the thermal evolution discussed above, strongly suggested the presence of organic moieties in the polycations. As indicated before, $[(TiO)_8(OH)_{12}]^{4+}$ has been frequently claimed as the intercalating polycationic Ti species, but this species was initially proposed for the hydrolysis of $TiCl_4$ with HCl, without the presence of organic compounds. Later, the hydrolysis of other Ti-compounds, mainly alkoxides, has been reported, and the incorporation of organic moieties to the polycations has been suggested (although without proposing other formulas) (Del Castillo et al., 1997; Vicente et al., 2001). The calcination of this solid led to an increase in SSA, reaching a value of 164 m^2/g for the pillared solid. This increase may be related to removal of such organic moieties, together with the elimination of water during the transformation from polycations to pillars. For comparative purposes, this solid was also calcined at 300 °C, showing at this temperature a S_{BET} of 115 m^2/g, consistent with a partial removal of the organic moieties.

Table 3
Basal spacing (Å) for intercalated and calcined samples.

	Intercalated	300 °C	500 °C
Mt	13.60		9.57
MtTi	19.63	19.20	18.60
MtTiFe5	19.64	18.33	–
MtTiFe10	21.19	17.19	16.99
MtTiCu5	18.92	18.29	–
MtTiCu10	21.14	16.57	16.49
MtTiCr5	22.03	16.57	–
MtTiCr10	22.88	17.39	16.03

Table 4
BET specific surface area (S_{BET}), external surface area (S_{ext}) and micropore volume (V_m) of natural montmorillonite and of the pillared solids.

	S_{BET} (m^2/g)	S_{ext} (m^2/g)	V_m (cm^3/g)
Mt	49	49	0.000
M-500	80	64	0.009
MtTi	97	55	0.023
MtTi-300	115	52	0.035
MtTi-500	164	80	0.047
MtTiFe10-500	300	114	0.103
MtTiCu10-500	329	135	0.108
MtTiCr10-500	272	124	0.082

Interestingly, the SSA of the doped-, PILC solids were remarkably higher than that of the solid pillared with only Ti, reaching a maximum value of 329 m^2/g for the solid doped with Cu, with the parallel increase in the porosity. Obviously, this high SSA cannot be only ascribed to the small incorporation of this element (0.51% expressed as CuO and referred to dried solid), but may be related to the changes that the presence of this element induced in the polymerization of Ti(IV), as commented above. So, the incorporation of the dopant cations induced an important increase in the textural properties, making these solids more potentially applicable.

The acidity of the solids was evaluated by adsorption of pyridine and further heating at increasing temperatures, following the process by FTIR spectroscopy. Typically, the pyridine bands were intense after adsorption and after heating at 100 and 200 °C, disappearing almost completely after calcination at 300 °C (Fig. 3). The results obtained are shown in Table 5.

For the parent Mt, the number of Brönsted and Lewis sites is similar (before pyridine adsorption, this solid was calcined at 500 °C, the same calcination temperature of the pillared solids). Compared to the natural clay, Brönsted sites concentration strongly increased in PILC, while that

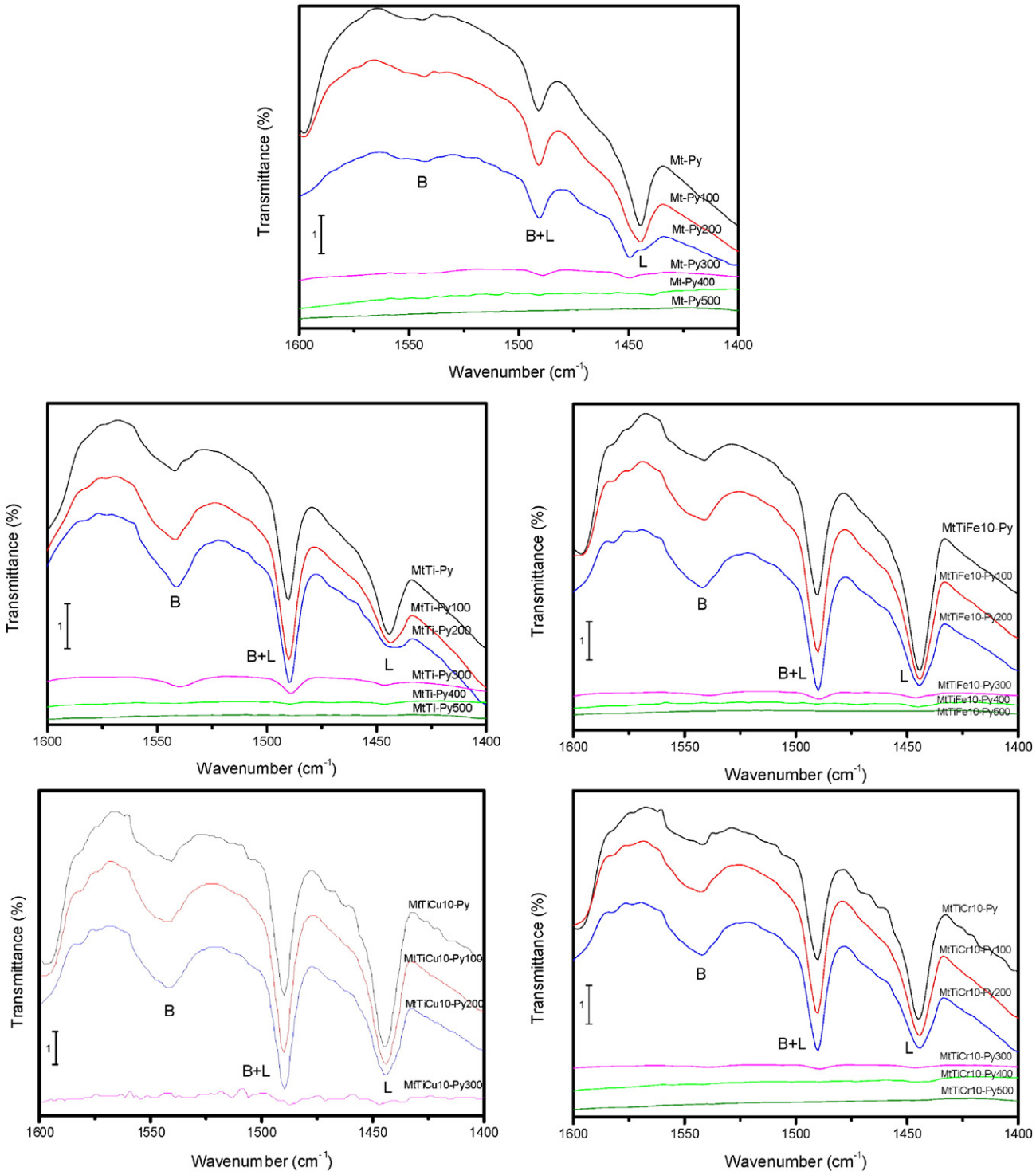

Fig. 3. FTIR spectra of the pillared solids after adsorption of pyridine and heating at increasing temperatures.

Table 5
Brönsted and Lewis acidity (μmol/g) of natural montmorillonite and of the pillared solids after adsorption of pyridine and heating at different temperatures. Between brackets, the number of acid centres per specific surface area unit (μmol/m^2).

	Room Temperature		100 °C		200 °C		300 °C	
	B	L	B	L	B	L	B	L
Mt	13.9 (0.174)	19.2 (0.240)	18.1 (0.226)	24.1 (0.301)	19.7 (0.246)	23.8 (0.297)	19.4 (0.243)	20.1 (0.251)
MtTi	58.2 (0.355)	1.9 (0.012)	76.3 (0.465)	2.4 (0.015)	87.4 (0.533)	2.6 (0.016)	82.3 (0.502)	2.1 (0.013)
MtTiFe	78.6 (0.262)	0	105.5 (0.352)	4.6 (0.015)	122.1 (0.407)	4.7 (0.016)	90.0 (0.300)	3.6 (0.012)
MtTiCu	70.0 (0.213)	0	168.3 (0.512)	4.8 (0.015)	184.0 (0.559)	5.7 (0.017)	0	0
MtTiCr	35.3 (0.130)	2.3 (0.008)	72.1(0.265)	6.5 (0.024)	82.7 (0.304)	7.0 (0.026)	81.6 (0.300)	6.4 (0.024)

of Lewis sites strongly decreased. In PILC, Brönsted sites are mainly associated to the pillars and to clay silanol groups, while Lewis sites are associated to exchangeable cations and Al^{3+} cations with incomplete coordination. In the PILC solids, the Brönsted sites bands were much more intense than those from Lewis sites, and consequently the number of sites was clearly higher.

As indicated, Lewis acidity decreased upon pillaring. Lewis sites associated to the exchangeable cations of the original clay must decrease with pillaring because a large amount of these cations, although not all, are replaced by polycations, making these sites to disappear, although pillaring may increase the number of Al^{3+} cations with incomplete coordination located in the layers edge, which become accessible to pyridine because of the layer separation during pillaring. In opposite, Brönsted acidity increased by a factor of 4–6, even surpassing the 150 μmol/g value. Such an increase can be due to two reasons, the increase in the number of silanol groups that became accessible to pyridine by the layer separation during pillaring, and the presence of this type of acidity in the pillars.

When analysing the effect of the doping elements, comparing the doped pillared solids to that pillared with only Ti, it was observed that the incorporation of Fe produced a remarkable increase of Brönsted acidity, while Cr had no significant effects. In the case of Cu, it produced a significant increase for the dried solid, and for those heated at 100 and 200 °C, but the complete disapparition of the acidity after heating at 300 °C. However, it should be taken into account that acidity is a surface property, and then it should be hardly related to the total mass of solid and instead, it should be referred to the surface area of the solid. On calculating the number of acid centres per m^2, the presence of the cationic dopants did not generate new acid centres but modified the strength of those already existing; in fact, sample MtTi showed the largest values of acidity per m^2 (Table 5). Doping with Fe^{3+} and Cr^{3+} produced a decrease of the acidity evaluable by pyridine adsorption, probably because pyridine cannot access to the micropores developed in the doped solids. However, in the case of Cu^{2+}, Brönsted acidity increased, although it disappeared at low temperature. This increase in Brönsted acidity can be tentatively assigned to undetectable by XRD particles of copper oxides present in the surface of the pillared clay.

4. Conclusions

Cations Cu^{2+}, Fe^{3+} or Cr^{3+} have been effectively incorporated into Ti-pillared Mt by adding these cations to the Ti solutions before polymerization. The presence of the doping elements strongly affected the polymerization of Ti, and although their amount in the final solids was low, up to 0.5%, the properties of the final pillared solids were strongly affected by their presence: the basal spacing of the doped Ti-PILC was 16–17 Å, lower than the spacing of the undoped Ti-pillared solid (18.60 Å), but while undoped Ti-PILC was almost delaminated, the doped solids were very well ordered. The amount of Ti fixed was higher in the doped solids, probably by the influence of the doping cations during the polymerization of titanium species. The specific surface area was also strongly larger for the doped solids than for the undoped one (272–329 m^2/g vs. 164 m^2/g for solids calcined at 500 °C). The incorporation of Fe or Cu produced an increase of the acidity, although in the Cu-solid it rapidly decreased with temperature.

Acknowledgements

The authors thank the support from the Spanish Ministry of Economy and Competitiveness (MINECO) and the European Regional Development Fund (FEDER) (grant MAT2013-47811-C2-R). BGR thanks a pre-doctoral grant from Universidad de Salamanca.

Appendix A. Supplementary data

Supplementary data to this article can be found online at http://dx.doi.org/10.1016/j.clay.2015.09.010.

References

Barbosa, L.V., Marçal, L., Nassar, E.J., Calefi, P.S., Vicente, M.A., Trujillano, R., Rives, V., Gil, A., Korili, S., Ciuffi, K.J., de Faria, E.H., 2015. Kaolinite–titanium oxide nanocomposites prepared via sol–gel as heterogeneous photocatalysts for dyes degradation. Catal. Today 246, 133–142.
Barzetti, T., Selli, E., Moscotti, D., Forni, L., 1996. Pyridine and ammonia as probes for FTIR analysis of solid acid catalysts. J. Chem. Soc. Faraday Trans. 92, 1401–1407.
Brunauer, S., Emmet, P.H.E., Teller, E., 1938. Adsorption of gases in multimolecular layers. J. Am. Chem. Soc. 20, 1553–1564.
Chmielarz, L., Kuśtrowski, P., Piwowarska, Z., Dudek, B., Gil, B., Michalik, M., 2009. Montmorillonite, vermiculite and saponite based porous clay heterostructures modified with transition metals as catalysts for the DeNOx process. Appl. Catal. B Environ. 88, 331–340.
Del Castillo, H.L., Gil, A., Grange, P., 1997. Influence of the nature of titanium alkoxide and of the acid of hydrolysis in the preparation of titanium-pillared montmorillonites. J. Phys. Chem. Solids 58 (1053), 1062.
Del Rey-Pérez-Caballero, F.J., Poncelet, G., 2000. Microporous 18 Å Al-pillared vermiculites: preparation and characterization. Microporous Mesoporous Mater. 37, 313–327.
Einaga, H., 1979. Hydrolysis of titanium(IV) in aqueous (Na,H)Cl solution. J. Chem. Soc. Dalton 1917-1919.
Emeis, C.A., 1993. Determination of integrated molar extinction coefficients for absorption bands of pyridine adsorbed on solid acid catalysts. J. Catal. 141, 347–353.
Gil, A., Vicente, M.A., Korili, S.A., Trujillano, R., 2010. Pillared Clays and Related Catalysts. Springer.
Greenwood, N.N., Earnshaw, A., 2012. Chemistry of the Elements. Butterworth–Heinemann.
Harvey, C.C., Lagaly, G., 2013. Industrial applications. In: Bergaya, F., Lagaly, G. (Eds.), Handbook of Clay Science, Second Edition, Part B: Techniques and Applications. Elsevier, Amsterdam, pp. 451–490.
Kocí, K., Matejka, V., Kovár, P., Lacny, Z., Obalová, L., 2011. Comparison of the pure TiO_2 and kaolinite/TiO_2 composite as catalyst for CO_2 photocatalytic reduction. Catal. Today 161, 105–109.
Lin, J.T., Jong, S.J., Cheng, S., 1993. A new method for preparing microporous titanium pillared clays. Microporous Mater. 1, 287–290.
Lippens, B.C., De Boer, J.H., 1965. Studies on pore systems in catalysis. J. Catal. 4, 319–323.
McCabe, R.W., Adams, J.M., 2013. Clay minerals as catalysts. In: Bergaya, F., Lagaly, G. (Eds.), Handbook of Clay Science, Second Edition, Part B: Techniques and Applications. Elsevier, Amsterdam, pp. 491–538.
Nakata, K., Fujishima, A., 2012. TiO_2 photocatalysis: design and applications. J. Photochem. Photobiol. C 13, 169–189.
Rightor, E.G., Tzou, M.S., Pinnavaia, T.J., 1991. Iron oxide pillared clay with large gallery height: synthesis and properties as a Fischer–Tropsch catalyst. J. Catal. 130, 29–40.
Rouquerol, F., Rouquerol, J., Sing, K., 1998. Adsorption by Powders and Porous Solids – Principles, Methodology and Applications. Academic Press.
Schneider, J., Matsuoka, M., Takeuchi, M., Zhang, J., Horiuchi, Y., Anpo, M., Bahnemann, D.W., 2014. Understanding TiO_2 photocatalysis: mechanisms and materials. Chem. Rev. 114, 9919–9986.

Stünzi, H., Marty, W., 1983. Early stage of the hydrolysis of chromium (III) in aqueous solution. Characterization of a tetrameric species. Inorg. Chem. 22, 2145–2150.
Vicente Rodríguez, M.A., Suárez Barrios, M., Bañares Muñoz, M.A., López González, J.D., 1996. Comparative FT–IR study of the removal of octahedral cations and structural modifications during acid treatment of several silicates. Spectrochim. Acta A 52, 1685–1694.
Vicente, M.A., Bañares-Muñoz, M.A., Toranzo, R., Gandía, L.M., Gil, A., 2001. Influence of the Ti precursor on the properties of Ti-pillared smectites. Clay Miner. 36, 125–138.
Vicente, M.A., Gil, A., Bergaya, F., 2013. Pillared clays and clay minerals. In: Bergaya, F., Lagaly, G. (Eds.), Handbook of Clay Science, Second Edition, Part A: Fundamentals. Elsevier, Amsterdam, pp. 523–557.
Yuan, G.D., Theng, B.K.G., Churchman, G.J., Gates, W.P., 2013. Clays and clay minerals for pollution control. In: Bergaya, F., Lagaly, G. (Eds.), Handbook of Clay Science, Second Edition, Part B: Techniques and Applications. Elsevier, Amsterdam, pp. 587–644.